AMERICAN JOURNAL OF PHYSICAL ANTHROPOLOGY 137:397–411 (2008)

Temporal Squama Shape in Fossil Hominins: Relationships to Cranial Shape and a Determination of Character Polarity

Claire E. Terhune[1]* and Andrew S. Deane[2]

[1]*Institute of Human Origins, School of Human Evolution and Social Change, Arizona State University, Tempe, AZ 85287-2402*
[2]*Department of Pathology and Anatomical Sciences, University of Missouri-Columbia, Columbia, MO 65212*

KEY WORDS *Homo erectus*; cranial morphology; High Resolution-Polynomial Curve Fitting (HR-PCF)

ABSTRACT In 1943, Weidenreich described the squamosal suture of *Homo erectus* as long, low, and simian in character and suggested that this morphology was dependent upon the correlation between the size of the calvarium and the face. Many researchers now consider this character to be diagnostic of *H. erectus*. The relationship between cranial size and shape and temporal squama morphology, however, is unclear, and several authors have called for detailed measurements of squamosal variation to be collected before any conclusions are drawn regarding the nature of the morphology observed in *H. erectus*. Thirteen fossil and extant taxa were examined to address two questions: 1) Are size and shape of the temporal squama correlated with cranial vault morphology? and 2) Is the *H. erectus* condition plesiomorphic? To answer these questions, measurements were collected and indices were calculated for squamosal suture height, length, and area in relation to metric variables describing cranial size and shape. A two-dimensional morphometric study was also completed using High Resolution-Polynomial Curve Fitting (HR-PCF) to investigate correlations between curvature of the squamosal suture and curvature of the cranial vault. Results of both analyses indicate that squamosal suture form is related to cranial size and shape. Furthermore, the plesiomorphic condition of the squamosal suture for hominins was identified as high and moderately arched; this condition is retained in *H. erectus* and is distinct from the great ape condition. It is suggested that this similarity is the result of increased cranial length without a corresponding increase in cranial height. Am J Phys Anthropol 137:397–411, 2008.

In his 1943 monograph of the Zhoukoudian *Sinanthropus* material, Weidenreich characterized the long, low temporal squama of *Sinanthropus* as "simian" in character. This assessment was based on his comparison of the Zhoukoudian crania to the results of work conducted by Schultz in 1915, who calculated a cranial length–height index for several populations of modern *H. sapiens* and extant apes. Since this initial description by Weidenreich, a long, low, unarched temporal squama has been considered diagnostic of *H. erectus* (Macintosh and Larnach, 1972; Rightmire, 1984, 1990; Stringer, 1984; Wood, 1984; Antón, 2003) and is described as the plesiomorphic character state for hominin[1] taxa (Andrews, 1984; Martinez and Arsuaga, 1997). This conclusion has been reinforced by several recent authors (Andrews, 1984; Stringer, 1984; Martinez and Arsuaga, 1997; Antón, 2003). These descriptions have primarily been based on visual inspection and comparison of great ape squamae, which are also low and unarched. However, few of these analyses have provided a quantitative comparison of the temporal squama of *H. erectus* with other fossil hominins.

Studies of the temporal squama that have been conducted have focused primarily upon extant great ape taxa (Schultz, 1915; Holloway and Shapiro, 1992) and variation in squamosal shape among modern humans from several geographic regions (Schultz, 1915; Schulter, 1976). Others (Rak, 1978; Kimbel and Rak, 1985) have examined the morphology of the temporal squama and asterionic regions in association with masticatory stress in *Paranthropus boisei* and *Australopithecus afarensis*. To date, however, few studies have attempted to elucidate the relationship between temporal squama size and shape and overall cranial morphology and/or the polarity of this character within hominins; as a result, a long, unarched temporal squama continues to be considered diagnostic for *H. erectus* (e.g., Antón, 2003; Rightmire et al., 2006). Furthermore the discoveries of several new *H. erectus* crania with more arched squamosal sutures and crania suggest that perhaps further analyses and quantification of this trait are needed (Abbate et al., 1998; Asfaw et al., 2002; Baba et al., 2003; Rightmire et al., 2006; Spoor et al., 2007).

Although there is little doubt of the general shape of the squamosal suture in *H. erectus*, the polarity of this

[1]As used here, the term hominin includes modern humans and fossil taxa more closely related to them than to any other extant taxon, and hominid refers of the genera *Homo*, *Pan*, *Gorilla*, and *Pongo*, and all descendants of their common ancestor.

*Correspondence to: Claire E. Terhune, Institute of Human Origins, School of Human Evolution and Social Change, Arizona State University, Box 872402, Tempe, AZ 85287-2402, USA.
E-mail: claire.terhune@asu.edu

Received 14 August 2007; accepted 8 May 2008

DOI 10.1002/ajpa.20882
Published online 9 July 2008 in Wiley InterScience (www.interscience.wiley.com).

TABLE 1. Definitions of measurements and indices used in this study

Abbreviation	Measurement/Index	Definition
CC	Cranial Capacity	Cubic centimeters.
VH	Vault Height	Projected height of the vault from porion, perpendicular to Frankfurt horizontal (FH).
ORH	Orbital Roof Height	Projected height of the orbital roof from porion, perpendicular to FH.
SH	Squamosal Suture Height	Maximum projected height of the squamosal suture from porion, perpendicular to FH.
SL	Squamosal Suture Chord Length	Maximum length of the temporal squama from incisura parietalis to the anterior most point of the temporal bone, parallel to FH.
GOL	Cranial Length	Glabella to opisthocranion.
BPO	Biporionic Breadth	Chord distance from porion to porion.
SLI	Squamosal Length Index	Squamosal suture length/cranial length (%).
THLI	Temporal Height/Length Index	Squamosal suture height/suture length (%).
SORI	Squamosal/Orbital Roof Height Index	Squamosal suture height/orbital roof height (%).
GEOM	Geometric mean	$\sqrt[3]{}$(Cranial length × biporionic breadth × vault height).

character state as well as the degree of similarity between the morphology observed in *H. erectus* and the great apes is unclear. Furthermore, the relationship between the low, unarched, temporal squama and the long, low cranium of *H. erectus* has not been investigated. In fact, the need for further analyses examining variation within this feature was noted by Stringer (1984), and subsequently reiterated by Brauer (1994), who stated that: "For these and further measurements of the squama height, extensive analyses of variation, including several hominid taxa, appear to be necessary first." To address this lack of comparative analyses of temporal squama morphology and to assess the significance of the morphology observed in *H. erectus*, this study was designed to quantify temporal squama size and shape in extant and fossil great apes and humans via craniometric and two-dimensional morphometric analyses and to assess the relationship between the temporal squama and the cranium. Two questions were addressed by this research: 1) Are size and shape of the temporal squama correlated with specific variations in cranial vault morphology in extant apes and fossil hominins? and 2) Is the morphology seen in *H. erectus* the plesiomorphic character state for hominins?

The first research question assessed the extent to which temporal squama size and shape are correlated with particular aspects of cranial morphology. More specifically, if temporal squama size and shape are related to cranial vault shape, then increases in cranial length, height, or curvature should be accompanied by a corresponding increase in length, height, or curvature of the squama. In contrast, if the dimensions of the temporal squama vary independently of vault dimensions, then there should be no correlation between cranial length and squamosal length, cranial height and squamosal height, or cranial curvature and squamosal curvature. In addition to describing and quantifying squamosal variation in extant and fossil taxa, evaluating these potential relationships between cranial vault and squamosal morphology is essential for determining the nature of evolutionary changes in squamosal shape in the fossil hominins. This is the goal of the second research question, which examines potential scenarios by which the observed variation in temporal squama morphology could have evolved.

MATERIALS AND METHODS

In this study, we examined variation in the size and shape of the temporal squama and cranial vault, where the term size refers to linear dimensions of the cranial vault (e.g., cranial height, squamosal length) as well as a general measure of cranial size, the geometric mean of cranial length, breadth, and width. Shape refers to the relative placement of particular features of the squama in relation to the cranial vault (e.g., squamosal length in relation to cranial length) as well as to the form of the squamosal suture and outline of the cranial vault. Note that we only evaluated the influence of the cranial vault on temporal squama morphology, primarily as a result of a general lack of *a priori* expectations for why the temporal squama may vary in relation to the morphology of the facial skeleton. All of the previous research regarding temporal squama morphology (Schultz, 1915; Weidenreich, 1943; Stringer, 1984; Brauer, 1994) has focused on the cranial vault, and as such we chose only to test those previously discussed correlations between temporal squama and cranial vault morphology. In addition, the lack of intact facial skeletons in the fossil sample (and particularly for *H. erectus*) made an analysis of the relationships between the temporal squama and the face impractical.

Two separate but complimentary analytical methods were used for this study: a craniometric analysis, which investigated temporal squama morphology using a series of linear dimensions and indices, and a polynomial curve fitting analysis, which compared the curvature of the squamosal suture and cranial vault.

For the craniometric analysis, multiple measures of temporal squama morphology were collected and indices were calculated in order to describe squamosal suture morphology in relation to a number of metric variables expressing overall cranial size and shape (Table 1, Fig. 1). Because of the dramatic increase in cranial height and expansion of the parietals in hominins (Kimbel et al., 2004), measuring squamosal height as a percentage of overall cranial height was deemed to be inappropriate, and therefore squamosal height was measured in relation to orbital roof height (ORH), a value which was found to be essentially the same for all taxa sampled (only *G. gorilla* and *P. pygmaeus* differed substantially for this variable). Consequently, squamosal height as measured against the orbital roof (SORI) is discussed here. Means and distributions of all craniometric variables were analyzed and compared for each taxon using a Kruskal-Wallis test with two-tailed multiple (*post hoc*) comparisons. This nonparametric alternative to ANOVA was chosen because of a lack of normality and unequal variances among samples. Sexual dimorphism in temporal squama morphology was also assessed in the extant

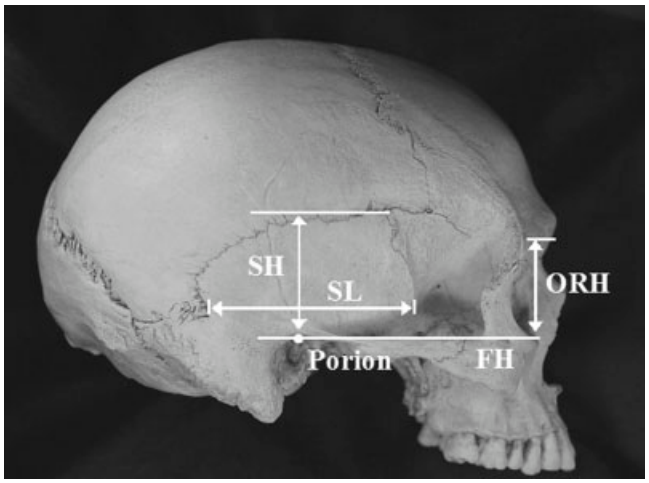

Fig. 1. Lateral view of a human cranium showing temporal squama measurements used in the craniometric analysis. SH, squama height; SL, squama length; ORH, orbital roof height; FH, Frankfurt horizontal.

taxa using two-sample *t*-tests, as were differences in temporal squama shape between Asian and African *H. erectus*. Correlations between variables describing squamosal and cranial size and shape were investigated using a two-tailed partial correlation analysis on the raw linear dimensions, where cranial size (as measured by the geometric mean) was held constant. All analyses were conducted using Microsoft Excel and Statistica (Statsoft).

To assess how the curvature of the cranium covaries with the curvature of the squamosal suture, a two-dimensional morphometric study using High Resolution-Polynomial Curve Fitting (HR-PCF) was also conducted to investigate the correlation between the second-order element of the curvature of the squamosal suture and the cranial vault (see Fig. 2). HR-PCF (Deane et al., 2005) is an alternative to traditional curvature quantification methods. It is independent of size and length, and, unlike traditional methods for curvature quantification, it avoids the assumption of curvature circularity by modeling curvature as a second-order polynomial ($Y = Ax^2 + Bx + C$). HR-PCF was used to generate second-order polynomial functions representing the second-order element of the cranial and squamosal curvatures. The resulting polynomial coefficients were then used as the raw variables in a discriminant function analysis (DFA). DFA was selected for its ability to identify patterns of correlation among variables and to determine which variables discriminate between two or more naturally occurring groups. Considering that group (i.e., taxon) membership is well understood for all individuals, DFA is the most appropriate statistic available for determining how variables differ between *a priori* taxonomic groupings. Standardized canonical discriminant function coefficients were used to compare the relative importance of the independent variables to each discriminant function. Means and distributions of all curvature variables were analyzed and compared for each taxon. Interspecific variation in the first polynomial coefficient (A) representing squamosal curvature, which was both normally distributed and shown to have equal variance, was examined for a subset of taxa with samples greater than $n = 5$ using a one-way ANOVA test with two-tailed multiple (*post hoc*) comparisons. A two-tailed Pearson's correlation analysis was also used to identify specific correlations between curvature variables. HR-PCF was conducted using software specifically written for HR-PCF analysis (Deane et al., 2005) and the DFA, ANOVA, and correlation analyses were conducted using SPSS (Jandel Scientific).

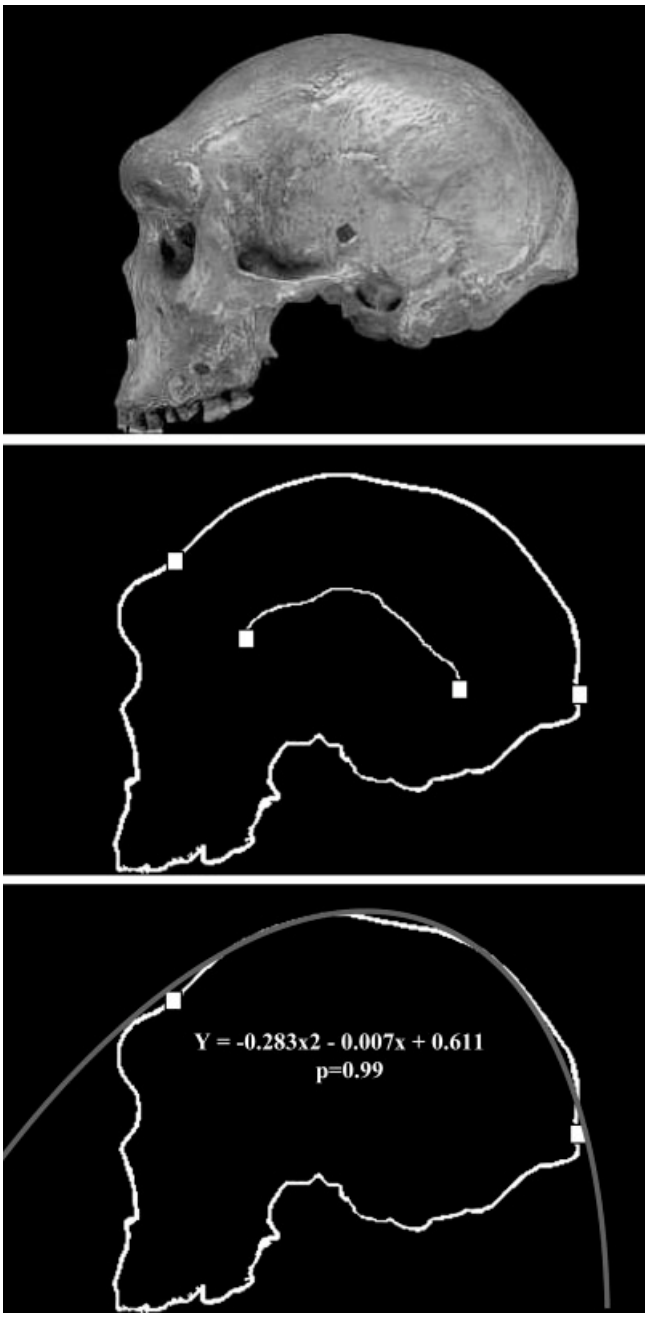

Fig. 2. Images demonstrating the three stages of HR-PCF analysis. (**A**) a digital image is generated for the specimen; (**B**) the image is reduced to a grayscale outline and markers are identified where there are discontinuities in the curvature outline or at points of inflection between curves. These markers are used to define the endpoints of the curve of interest; (**C**) a second order polynomial function ($Y = Ax^2 + Bx + C$) is fitted to the selected curve; the individual polynomial coefficients are then used as independent variables in a multivariate statistical analysis.

TABLE 2. Fossil specimens used in this study

Taxon	Specimens	
A. afarensis:	AL 444-2[a,27]	Composite *A. afarensis*[b,c]
A. africanus:	Sts 5[c,4,12,27]	MLD 37/38[a,12,27]
	Sts 71[a,12,27]	Stw 505[16,17]
P. aethiopicus:	KNM-WT 17000[c,27]	
P. boisei:	OH 5[a,4,12,28]	KNM-ER 13750[c,27]
	KNM-ER 406[c,4,7,27]	
H. habilis (sensu lato):	OH 24[a,9,12]	KNM-ER 1470[a,12,18]
	KNM-ER 1813[c,12,18]	
H. erectus (sensu lato):	OH 9[c,6,12,21]	Sambungmacan 1[c,21,26]
	KNM-ER 3733[c,12,18,21]	Sambungmacan 3[20,21,22]
	KNM-ER 3883[a,12,18,25]	Dmanisi 2280[23,28]
	KNM-WT 15000[a,13,25]	Sangiran 2[c,12,21,23]
	Zhoukoudian III[a,2,14,18]	Sangiran 17[c,12,21,23]
	Zhoukoudian X[a,2,14,18]	Ngandong 6[a,21,23]
	Zhoukoudian XI[c,2,14,18]	Daka[b,19]
	Zhoukoudian XII[c,2,14,18]	KNM-ER 42700[b,30]
	Zhoukoudian Composite[b,c]	
H. heidelbergensis:	Steinheim[a,6,11]	Atapuerca 5[b,15]
	Narmada[a,11,18]	Petralona[b,15]
	Kabwe[c,18]	Dali[b,15]
	KNM-ES 11693[10,24]	Jiniushan[b,c]
	LH 18[a,18]	
	Atapuerca 4[b,15]	
H. neanderthalensis:	La Ferrassie [8,11,15]	Gibraltar (Forbes Quarry)[b,24]
	La Chapelle-aux-Saints[c,8,11]	Guattari[b,24]
	Amud 1[a,8]	
	Saccopastore[8,11,15]	
Anatomically Modern *H. sapiens* (AMHS):	Skhul V[c,5,8]	Predmosti II[a,24]
	Qafzeh 9[a,8]	Herto[b,29]
	Cro-Magnon 1[c,3,11]	Liujian[b,c]
	Jebel Irhoud 1[a,8]	Zhoukoudian Upper Cave 103[a,24]
	Fish Hoek[1,24]	Abri Pataud 1[b,24]

[a] Craniometric analysis only.
[b] 2D morphometric analysis only.
[c] Specimen photographed for this study.
Portions of the craniometric data and published images for the fossil specimens were compiled from: (1) Keith, 1931; (2) Weidenreich, 1943; (3) Vallois and Billy, 1965; (4) Tobias, 1967; (5) Suzuki and Takai, 1970; (6) Olivier and Tisier, 1975; (7) Leakey and Leakey, 1978; (8) Holloway, 1985; (9) Tobias, 1985; (10) Brauer and Leakey, 1986; (11) Kennedy et al., 1991; (12) Wood, 1991; (13) Walker, 1994; (14) Wu and Poirier, 1995; (15) Johanson and Edgar, 1996; (16) Conroy et al., 1998; (17) Lockwood and Tobias, 1999; (18) Holloway, 2000; (19) Asfaw et al., 2002; (20) Broadfield et al., 2001; (21) Delson et al., 2001; (22) Marquez et al., 2001; (23) Antón, 2002; (24) Schwartz and Tattersall, 2003; (25) Vekua et al., 2002; (26) Baba et al., 2003; (27) Kimbel et al., 2004; (28) Rightmire et al., 2006; (29) White et al., 2006; (30) Spoor et al., 2007.

Samples for the craniometric analysis included 43 fossil and 60 extant specimens; for the two-dimensional HR-PCF analysis, 37 fossil and 72 extant specimens were examined (Tables 2 and 3). The composition of these datasets differs as a result of specimen availability and completeness; for the craniometric analysis, measurements had to be taken directly on fossil specimens (or casts of fossils) or had to be available in the literature, whereas published photographs could also be included in the HR-PCF analysis. Data for the craniometric analysis were obtained by C.T. both through the literature and through direct measurements on cast (and some original comparative) specimens housed at the Institute of Human Origins (IHO) at Arizona State University and the Cleveland Museum of Natural History (CMNH); these data are available upon request to the authors. All measurements of cranial capacity were taken from the literature or were on file at the CMNH. For the curvature analysis, all images of original extant specimens were collected by A.D., and photos of fossil cast specimens were taken by A.D. and C.T. The images representing fossil taxa used in this study are either of high resolution casts housed at the University of Toronto and the Institute of Human Origins at Arizona State University, or were taken directly from the literature. All images were digitized by A.D. HR-PCF is a robust curvature quantification technique that is largely independent of the effects of parallax error. To demonstrate this, a two part controlled error study was conducted. In the first stage of the error study, the cranial curvature of a single specimen (*P. paniscus*) was analyzed from variable distances (range: 30–60 cm; interval: 10 cm) and heights (range: 4–9 cm; interval: 2.5 cm). Although there was slight variation among the resulting first (*A*) and third (*C*) coefficients, this was generally minimal (i.e., <5%)

TABLE 3. Extant samples used in this study

Taxon	Craniometric	2D Morphometric
P. pygmaeus	4 male, 4 female	8 male, 7 female
G. gorilla	9 male, 9 female	8 male, 7 female
P. troglodytes	9 male, 8 female	8 male, 7 female
H. sapiens	7 male, 10 female	17 male, 10 female[a]

[a] 2D images of 6 male and 1 female *H. sapiens* specimens were collected from Johanson and Edgar, 1996. Images were generated from the original specimens for all other extant specimens used in this study.

TABLE 4. Results generated from a controlled HR-PCF error study

	1st Coefficient (*A*)		2nd Coefficient (*B*)		3rd Coefficient (*C*)	
	Cranial	Squamosal	Cranial	Squamosal	Cranial	Squamosal
Stage 1						
Pan paniscus						
% Error[a]	3.807%		102.5%		4.53%	
Minimum value	0.2813		0.0035		0.2599	
Maximum value	0.3309		0.0460		0.3165	
Stage 2						
Homo sapiens #1						
% Error	4.46%	2.09%	47.74%	11.81%	2.75%	2.4%
Minimum value	0.3901	0.5644	0.0023	0.1179	0.4674	0.5044
Maximum value	0.4483	0.6302	0.0324	0.061	0.4095	0.5336
Homo sapiens #2						
% Error	2.619%	2.43%	61.41%	119.24%	3.43%	2.35%
Minimum value	0.4567	0.6514	0.0007	0.0028	0.4456	0.5495
Maximum value	0.5055	0.7087	0.0523	0.0403	0.4994	0.6080
Homo sapiens #3						
% Error	2.75%	3.5%	61.17%	62.17%	3.13%	2.82%
Minimum value	0.4622	0.5706	0.0016	0.0051	0.4433	0.4299
Maximum value	0.4976	0.6302	0.0199	0.0473	0.4897	0.4763

[a] % error represents the average % difference between individual coefficient values and a group mean.

and demonstrates that variation in the location of the camera does not significantly impact these coefficients (Table 4). Similar results were obtained from the second stage of the controlled error study where three extant specimens (*H. sapiens*) were photographed on 10 separate occasions and all set-up protocols were repeated prior to each photograph. Variation in the first (*A*) and third (*C*) polynomial coefficients representing cranial and squamosal curvature were minimal (i.e., <5%). The results generated in Stage II for the first and third coefficients demonstrate the relatively low risk for type II error during repeated simulated trials. In both stages of the error study, the observed error in the second coefficient (*B*) was substantially greater; ~102.5% for stage I and ranging between 11.81 and 119.24% in stage II (Table 4). The relatively high margins of error reported for the second coefficients in both stages are due in large part to the absolutely smaller coefficient values and suggest that while error expressed as a percentage difference between a given value and the group mean is high, the absolute difference between a given value and the group mean is considerably small. Consequently, a margin of error expressed as an average percent difference between individual coefficient values and a group mean for the second coefficient does not accurately represent the magnitude of absolute variation within that coefficient and is therefore not likely to represent a systematic source of measurement error. Furthermore, given that the first coefficient (*A*) in a second order polynomial function is the most valuable as it expresses the nature of the curvature itself, and the second and third reflect only aspects of the orientation of that curve with respect to a standardized axes, it is unlikely that the relative margin of error reported for the second coefficient (*B*), if it were to represent a true source of error, will significantly impact HR-PCF analyses.

Of the 37 fossil specimens included in this study, 21 are represented by published images taken from the literature. Original images representing extant taxa were collected from the Royal Ontario Museum (ROM, Toronto, Canada), the American Museum of Natural History (AMNH, New York, USA), the National Museum of Natural History (NMNH, Washington D.C., USA), and the Royal Museum for Central Africa (RMCA, Tervuren, Belgium). Cranial curvature was defined as the distance between the most inferior point posterior to the supraorbital torus and the external occipital protuberance or superior nuchal line. Squamosal curvature is defined as a line between the point where the squamosal suture crosses the superior border of the zygomatic arch in lateral view and the parietal notch (Figs. 1 and 2).

RESULTS

Craniometric analysis

Visual inspection of the data indicate that the great apes had the shortest[2] and widest squamae while the humans had the tallest and narrowest temporal squamae as measured by SORI, SLI, and THLI (Table 5, Figs. 3–5). Of the great apes, *Pan troglodytes* had the shortest (although not the widest) temporal squama, whereas *Pongo pygmaeus* had the tallest. All of the extant samples (including humans) showed sexual dimorphism in temporal squama height, with males having a relatively higher squama than females. However, none of these differences were statistically significant when evaluated using a two-sample *t*-test. The variable THLI, which summarizes the relationship between height and length of the squama, indicates that *Gorilla* and *Pan* have the shortest, widest squamae, whereas the temporal squamae of *Pongo* and *Homo* were relatively taller and narrower. This result reflects the distinctive nature of the *Pongo* and *Homo* crania, which are themselves relatively anteroposteriorly (AP) narrow and superoinferiorly (SI) taller than those of the African apes. However, while the squama of *Pongo* is qualitatively distinct from the African apes, it is not statistically significantly different from *Gorilla* and *Pan*, although each of the great ape values are statistically different from the condition observed in *Homo* (Table 6).

Of the fossil hominins, the Neandertal and *H. erectus* samples had the smallest SORI values, and therefore the shortest squamae, while *A. afarensis* and *P. boisei* had the tallest squamae. Notably, the SORI value for *A. afarensis* (which for this variable only includes the specimen

TABLE 5. Species means for the temporal squama measurements used in the craniometric analysis

Taxon		SH	SL	SORI	SLI	THLI
P. pygmaeus	*N*	8	8	8	8	8
	Mean	30.93	55.92	83.52	45.43	55.98
	St Dev	5.52	6.81	17.38	6.37	11.81
G. gorilla	*N*	18	18	18	18	18
	Mean	33.19	76.50	73.94	46.97	43.55
	St Dev	5.41	7.56	11.28	3.45	6.69
P. troglodytes	*N*	17	17	17	17	17
	Mean	24.57	56.19	56.35	40.74	43.85
	St Dev	3.35	4.71	7.13	2.41	5.55
A. afarensis	*N*	2	2	1	2	2
	Mean	51.50	69.50	142.86	43.63	75.08
	St Dev	6.36	7.78	n/a	7.18	17.56
A. africanus	*N*	4	4	4	3	4
	Mean	35.75	58.75	102.73	40.55	63.06
	St Dev	2.75	10.81	20.19	6.29	17.12
A. boisei	*N*	3	3	3	3	3
	Mean	46.00	73.33	129.02	44.24	62.81
	St Dev	5.29	7.23	16.57	3.75	5.01
A. aethiopicus	*N*	1	1	1	1	1
	Mean	39.00	71.00	111.43	48.30	54.93
	St Dev	n/a	n/a	n/a	n/a	n/a
H. habilis	*N*	3	3	3	3	3
	Mean	36.33	52.67	105.76	34.26	69.06
	St Dev	4.16	6.66	5.04	1.87	1.01
H. erectus	*N*	14	14	14	14	14
	Mean	41.21	71.57	102.63	37.50	57.92
	St Dev	4.66	6.49	15.88	3.02	7.40
H. heidelbergensis	*N*	5	5	5	5	5
	Mean	47.80	70.20	114.24	35.61	68.38
	St Dev	5.17	6.79	13.67	2.12	7.58
H. neanderthalensis	*N*	4	4	4	4	4
	Mean	41.13	62.00	94.95	30.82	66.42
	St Dev	3.33	4.69	8.07	2.58	4.62
AMHS	*N*	7	7	7	7	7
	Mean	47.57	68.29	109.94	34.61	70.07
	St Dev	3.78	6.39	10.33	2.48	7.39
H. sapiens	*N*	17	17	17	17	17
	Mean	48.12	66.52	121.12	36.65	72.62
	St Dev	5.27	6.62	15.61	2.66	7.52

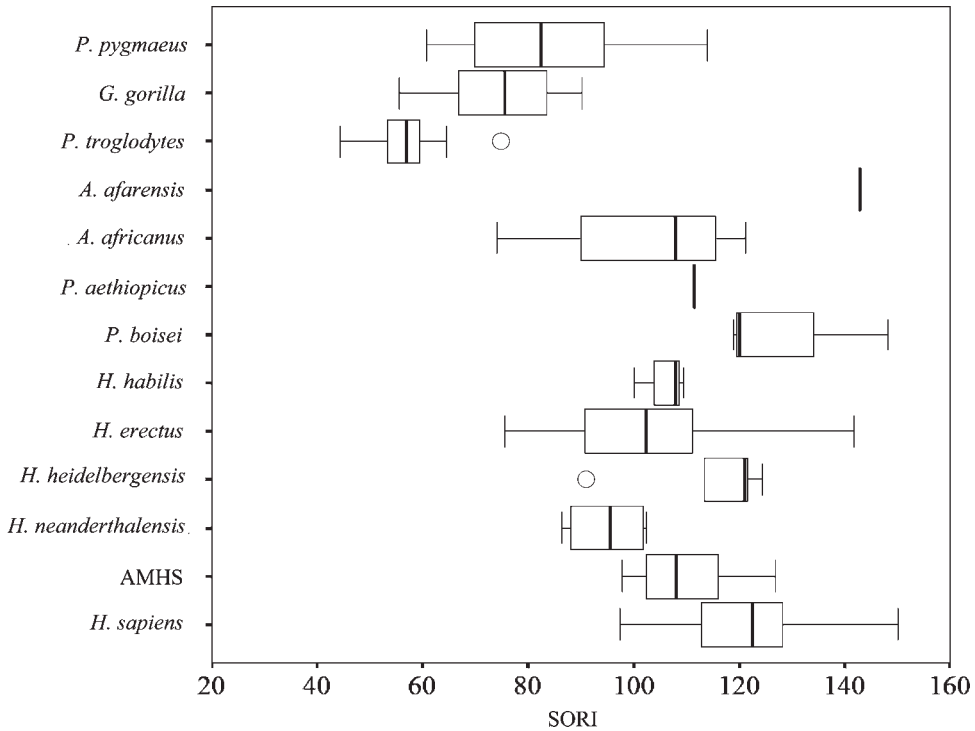

Fig. 3. Box plot of squamosal-orbital roof index (SORI) values for the extant and fossil taxa. For this analysis, the composite *A. afarensis* was excluded, making the value for *A. afarensis* a single data point. Note the general dissimilarity between the values obtained for the great apes as compared to the values for the hominin species, as well as the very high values obtained for *A. afarensis* and *P. boisei*. Darkened bars represent the median value for each group, while the boxes show the interquartile range, from the 25th to the 75th percentile, and the whiskers extend to data within the 1.5 times the interquartile range. Outliers are designated by open circles.

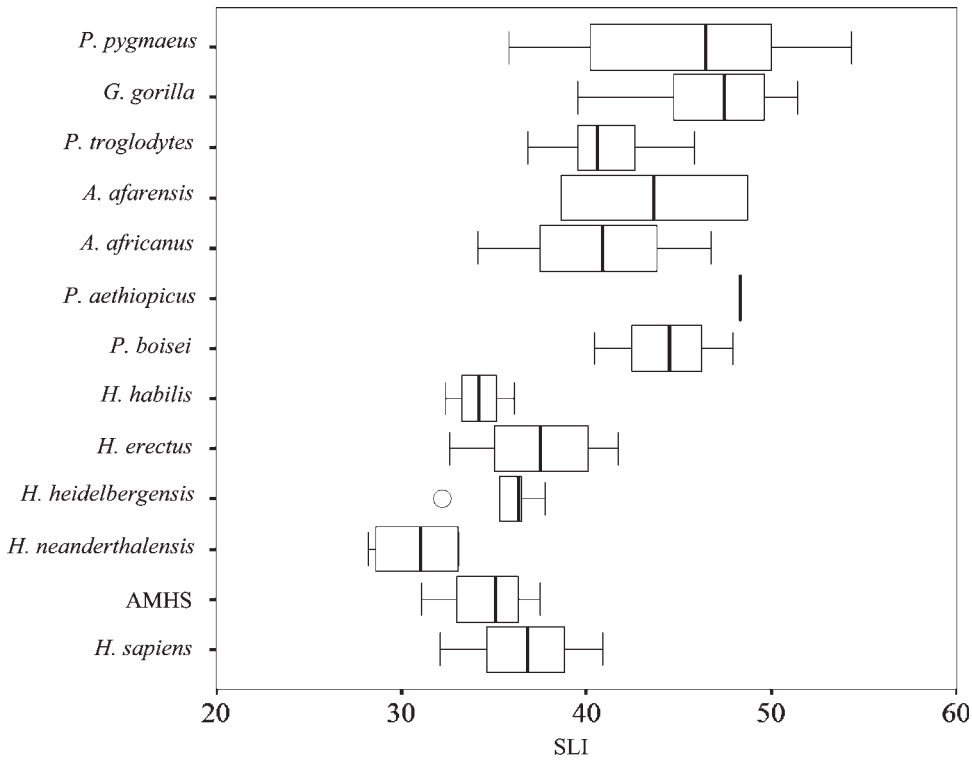

Fig. 4. Box plot of squamosal length index (SLI) values for the extant and fossil taxa.

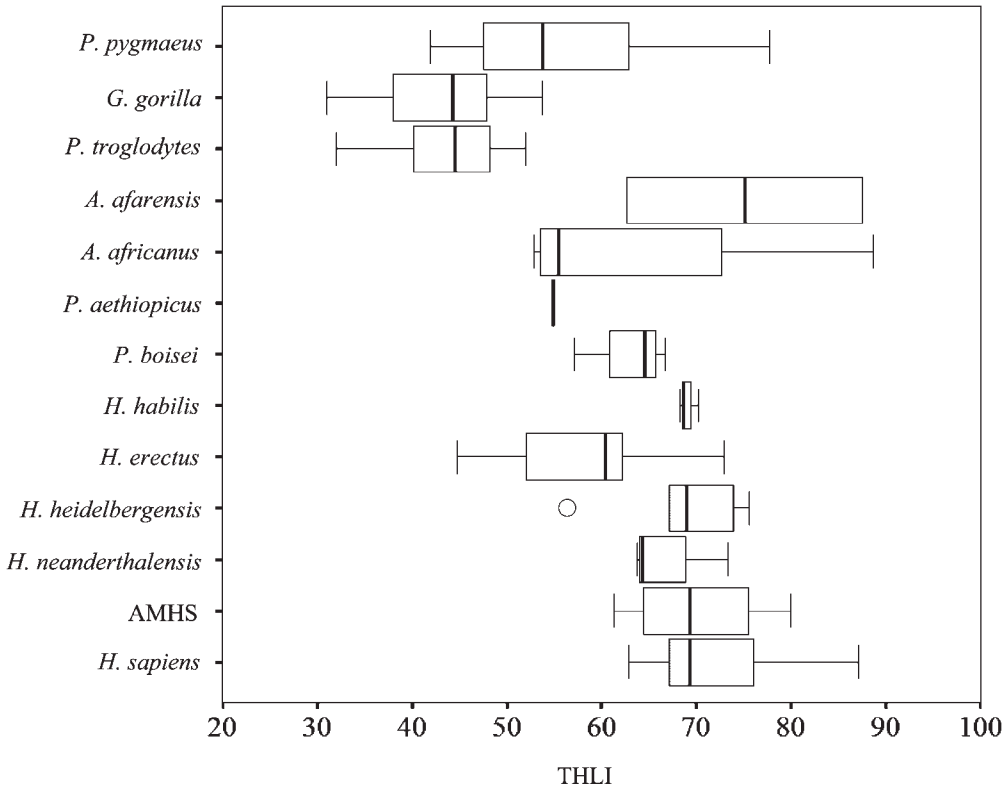

Fig. 5. Box plot of temporal squama height/length index (THLI) values for the extant and fossil taxa.

AL 444-2) was among the highest of all the SORI values measured. This may be a result of postmortem deformation of this specimen (Kimbel et al., 2004), although several *P. boisei* specimens also display similarly high SORI values.

TABLE 6. Results of the Kruskal-Wallis test for SORI, SLI, and THLI and the accompanying matrices showing the corrected P*-values for the significance test between groups in bold*

	A. africanus	*A. boisei*	*H. habilis*	*H. erectus*	*H. heidelbergensis*	*H. neanderthalensis*	AMHS	*P. pygmaeus*	*G. gorilla*	*P. troglodytes*
SORI: Kruskal-Wallis test: H (df = 10, N = 100) =77.40, $P < 0.0001$										
A. boisei	1.000									
H. habilis	1.000	1.000								
H. erectus	1.000	1.000	1.000							
H. heidelbergensis	1.000	1.000	1.000	1.000						
H. neanderthalensis	1.000	1.000	1.000	1.000	1.000					
AMHS	1.000	1.000	1.000	1.000	1.000	1.000				
P. pygmaeus	1.000	0.852	1.000	1.000	1.000	1.000	1.000			
G. gorilla	1.000	0.064	1.000	0.134	0.057	1.000	0.073	1.000		
P. troglodytes	0.094	**0.001**	0.206	<**0.001**	<**0.001**	0.743	<**0.001**	1.000	1.000	
H. sapiens	1.000	1.000	1.000	1.000	1.000	1.000	1.000	**0.043**	<**0.001**	<**0.001**
SLI: Kruskal-Wallis test: H (df = 10, N = 99) = 66.45, $P < 0.0001$										
A. boisei	1.000									
H. habilis	1.000	0.797								
H. erectus	1.000	1.000	1.000							
H. heidelbergensis	1.000	1.000	1.000	1.000						
H. neanderthalensis	1.000	0.089	1.000	1.000	1.000					
AMHS	1.000	0.381	1.000	1.000	1.000	1.000				
P. pygmaeus	1.000	1.000	0.188	0.331	0.184	**0.005**	**0.019**			
G. gorilla	1.000	1.000	**0.012**	**0.001**	**0.004**	<**0.001**	<**0.001**	1.000		
P. troglodytes	1.000	1.000	1.000	1.000	1.000	**0.040**	0.163	1.000	0.747	
H. sapiens	1.000	1.000	1.000	1.000	1.000	1.000	1.000	**0.039**	<**0.001**	0.343
THLI: Kruskal-Wallis test: H (df = 10, N = 100) =73.25, $P < 0.0001$										
A. boisei	1.000									
H. habilis	1.000	1.000								
H. erectus	1.000	1.000	1.000							
H. heidelbergensis	1.000	1.000	1.000	1.000						
H. neanderthalensis	1.000	1.000	1.000	1.000	1.000					
AMHS	1.000	1.000	1.000	1.000	1.000	1.000				
P. pygmaeus	1.000	1.000	1.000	1.000	1.000	1.000	1.000			
G. gorilla	0.838	1.000	0.074	0.198	**0.009**	0.107	**0.001**	1.000		
P. troglodytes	0.862	1.000	0.077	0.220	**0.009**	0.113	**0.001**	1.000	1.000	
H. sapiens	1.000	1.000	1.000	0.139	1.000	1.000	1.000	0.300	<**0.001**	<**0.001**

Significant P-values are in bold.

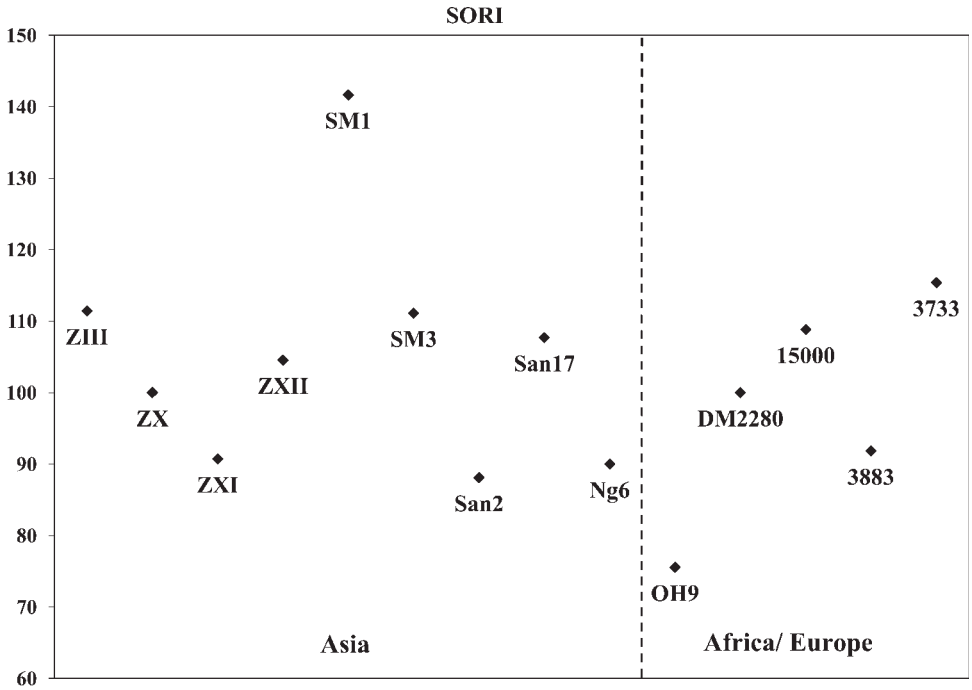

Fig. 6. Scatterplot of SORI values for the *H. erectus* sample showing the distribution of values by geographic region.

In anteroposterior dimensions, Neandertals also had the narrowest temporal squama (i.e., SLI value), indicating that the temporal squama as a whole takes up a much smaller percentage of the cranial vault than in other hominin taxa; whether this result is related to an increase in cranial vault size or a decrease in temporal squama size is unclear. The SLI values for *H. erectus*, in contrast, were generally consistent with those measured for most of the *Homo* species, although the observed range of values for *H. erectus* considerably overlapped the distributions for *Pan*, *A. afarensis*, and, *A. africanus*. THLI values for the hominin taxa were higher than the values observed for the apes, indicating that hominins have a higher and narrower (AP) squama on average. However, very low THLI values were observed for *A. africanus*, *P. aethiopicus*, and *H. erectus*. Furthermore, the distribution of THLI values for *H. erectus* did extend into the range of observed THLI values for the African apes.

The results of the Kruskal-Wallis test with multiple comparisons indicated that there are indeed statistical differences between the samples in temporal squama shape (note that *A. afarensis* and *P. aethiopicus* were excluded from this analysis because of their small sample sizes) (Table 6). Relative squama length differs significantly between *G. gorilla* and all species of *Homo*; *P. pygmaeus* is also distinct from several *Homo* species in squama length (*H. neanderthalensis*, AMHS, and *H. sapiens*, but not *H. erectus* or *H. habilis*), and *Pan* is only distinct from Neandertals, who have significantly narrower squamae than *Pan*. This suggests that, at least in relation to *Pan*, squama length is relatively stable across hominin species (although this may be an artifact of sample size). For SORI value, *Pan* is significantly different from all of the hominin taxa, except for *A. africanus*, *H. habilis*, and *H. neanderthalensis*. However, the *P*-values for the former two comparisons (*Pan* vs. *A. africanus* and *H. habilis*) approach significance ($P = 0.09$ and $P = 0.2$), whereas the *P*-value for the comparison between *Pan* and Neandertals is very high ($P = 0.74$); thus, it is possible that small sample sizes decreased the statistical power in the first two comparisons, while the value for the *Pan* vs. Neandertal comparison suggests that there is no significant difference in squama height in these two taxa regardless of sample size issues. Finally, the THLI values differ significantly only for *Gorilla* and *Pan* vs. *H. heidelbergensis*, AMHS, and *H. sapiens*. However, the differences between *Gorilla* and *Pan* vs. *H. habilis* and *H. neanderthalensis* both approach significance, potentially suggesting that if the sample sizes were larger for these taxa, they may indeed be statistically significantly different in this index value.

Although all of the African and Asian *H. erectus* specimens were considered here as part of the same species, in order to investigate the distribution of values within this sample the values for the African and Asian *H. erectus* specimens were also examined separately. Results indicated that specimens from each geographic region did not consistently cluster with one another in measures of temporal size or shape (see Fig. 6), and two-sample *t*-tests failed to find a significant difference between the African (including DM 2280) and Asian *H. erectus* samples in SORI, SLI, or THLI values.

When the geometric mean is held constant (e.g., size is controlled), there are several interesting correlations among the raw dimensions of the temporal squama and vault (Table 7). First, there is a significant positive correlation between CC and VH ($r = 0.774$, $P < 0.001$); this is most plausibly explained as an increase in cranial vault height as a result of expansion of the brain during hominin evolution. Vault height is also significantly positively correlated with squamosal height ($r = 0.331$, $P < 0.001$), which suggests that, when size is controlled for, the height of the squama does indeed increase as a result of an increase in cranial height. In addition, VH is negatively correlated with squamosal length ($r = -0.553$, $P < 0.001$). This relationship, as well as the negative correla-

tion between SL and CC ($r = -0.511$, $P < 0.001$), and the positive correlation between SL and BPO ($r = 0.512$, $P < 0.001$), seems most plausibly to be a result of the correlations between BPO, CC, and VH (BPO vs. CC: $r = -0.859$, $P < 0.001$, BPO vs. VH: $r = -0.841$, $P < 0.001$). In other words, increased cranial capacity during hominin evolution resulted in increased vault height, as well as smaller biporionic breadth (in relation to cranial capacity and vault height), and this relationship seems to be the driving factor for the aforementioned correlations between SL and CC and SL and BPO.

TABLE 7. Partial correlation analysis results between cranial and squamosal size and shape variables

	CC	VH	SH	SL	GOL
VH	**0.774**				
	***P*< 0.001**				
SH	0.188	**0.331**			
	$P = 0.074$	***P* = 0.001**			
SL	**−0.511**	**−0.553**	−0.069		
	***P*< 0.001**	***P*< 0.001**	$P = 0.490$		
GOL	0.072	−0.24	−0.104	0.252	
	$P = 0.50$	$P = 0.016$	$P = 0.301$	$P = 0.011$	
BPO	**−0.859**	**−0.841**	−0.269	**0.512**	−0.261
	***P*< 0.001**	***P*< 0.001**	$P = 0.007$	***P*< 0.001**	$P = 0.009$

Bolded correlations are significant after Bonferroni correction (critical alpha = 0.05/15 = 0.003). See Table 1 for variable abbreviations.

HR-PCF curvature analysis

Discriminant function analysis (DFA) of the dataset representing the second-order polynomial functions defining squamosal and cranial curvature was performed to determine which curvature variables discriminate between taxonomic groups. Figure 7 is a scatter plot of DF1 and DF2, which explain 93.0% of the total variation within the sample. DF1 (86.9% of variation, $P < 0.01$) represents an increase in both cranial curvature and squamosal curvature and a general separation of taxa with low and high degrees of curvature, although there is a small degree of overlap between those groups. Similarly, all *Australopithecus*, *Paranthropus*, early *Homo*, and *H. erectus* specimens cluster together and are generally separate from the cluster of later *Homo* species (*H. heidelbergensis*, *H. neanderthalensis*, and *H. sapiens*). This latter group is characterized by more pronounced squamosal and cranial curvatures. Discriminant function two represents only a general decrease in the degree of cranial curvature as well as a much smaller portion of the total sample variation (6.1% of variation, $P < 0.01$). There is little meaningful segregation of taxa along this axis, however; only KNM-WT 17000 (*P. aethiopicus*) is separated from all other taxa by that specimen's low and uncurved cranium.

Variation among taxa in the values of the first coefficient (A), the most informative coefficient for examining curvature, is illustrated in Figures 8 and 9 for cranial and squamosal curvature, respectively. As these figures demonstrate, there is considerable variation in squamosal curvature within hominin groups, but for the most part,

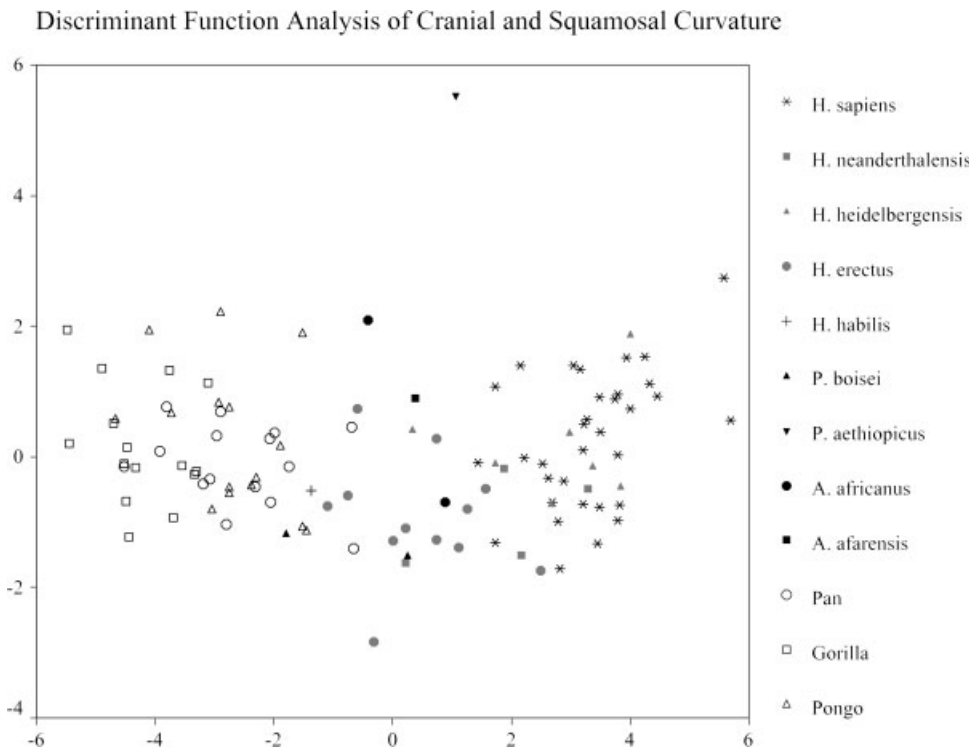

Fig. 7. Scatterplot of discriminant function coefficients derived from a multivariate analysis of second order polynomial coefficients ($Y = Ax^2 + Bx + C$) representing the second order element of cranial and squamosal curvature in the HR-PCF sample. Discriminant function 1 represents 86.9% of the total variance and represents an increase in the second order element of cranial and squamosal curvature such that extant hominids are the least curved, later *Homo* is the most curved and *Australopithecus*, *Paranthropus*, and Early *Homo* are intermediate. Discriminant function 2 represents 6.1% of the total variance.

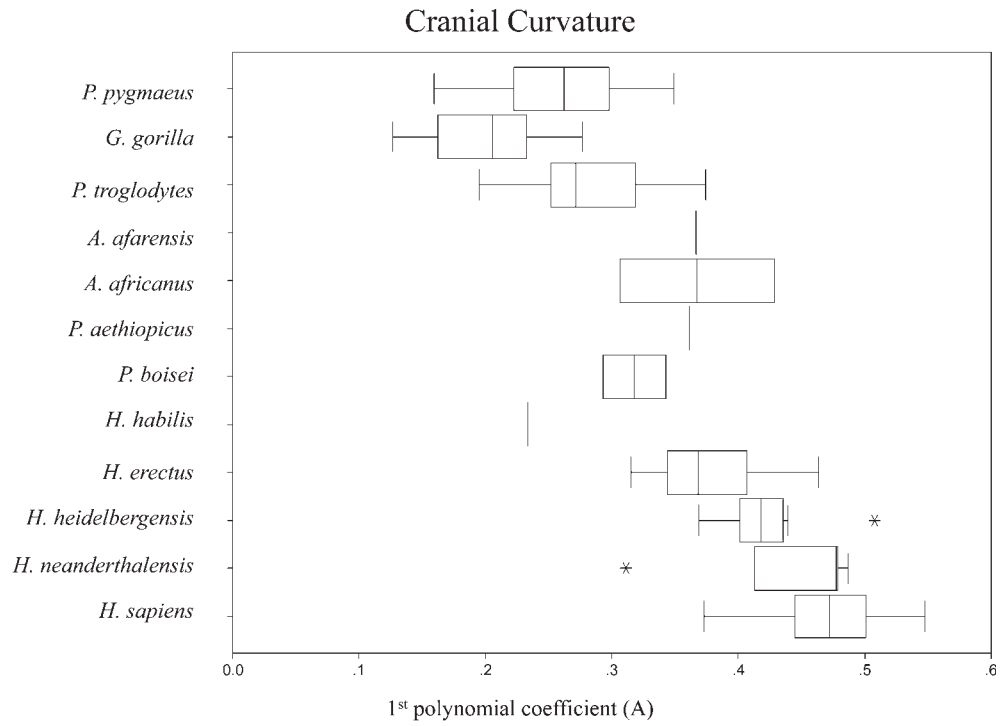

Fig. 8. Box plot of cranial curvature represented by the first coefficient (*A*) for the extant and fossil taxa. Outliers are indicated by asterisks.

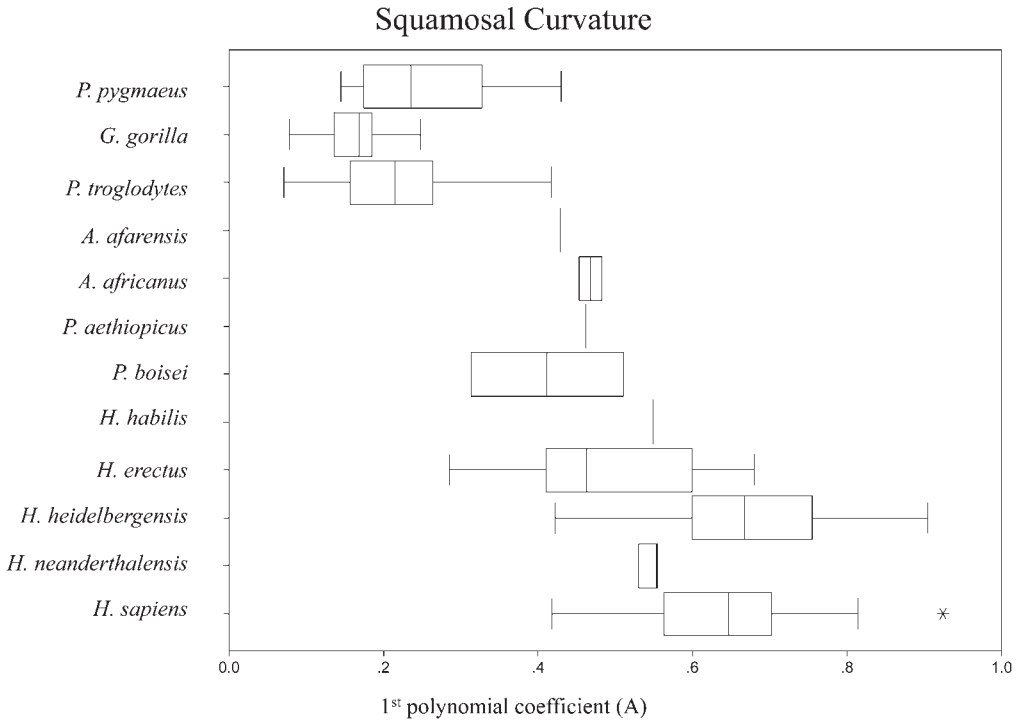

Fig. 9. Box plot of squamosal curvature represented by the first coefficient (*A*) for the extant and fossil taxa. Outliers are indicated by asterisks.

hominins are differentiated from the great apes by their considerably higher cranial and squamosal curvature values. In particular, the range of values for *H. erectus* overlaps considerably with the great ape condition, as was noted for the squamosal height measures discussed above. Regardless, a one-way ANOVA with multiple comparison tests identified statistically significant differences between the squamosal curvatures of apes and all fossil hominins ($P < 0.001$). In general, the mean squamosal curvature values for all fossil hominins are not statisti-

TABLE 8. Bonferonni and Tukey test significance values from the one-way ANOVA of extant hominid and fossil hominin squamosal curvature

	Apes	*H. erectus*	*H. heidelbergensis*	*H. neanderthalensis*
H. erectus	**<0.001/<0.001**	–	–	–
H. heidelbergensis	**<0.001/<0.001**	**0.004/0.005**	–	–
H. neanderthalensis	**<0.001/<0.001**	0.896/1.00	0.224/0.373	–
H. sapiens	**<0.001/<0.001**	**0.001/0.001**	0.899/1.00	0.378/0.745

Bonferonni values are on the left and Tukey values are on the right. Significant *P*-values are in bold.

TABLE 9. Correlation analysis results for squamosal and cranial curvature variables

	Cranial (*A*)	Cranial (*B*)	Cranial (*C*)	Squamosal (*A*)	Squamosal (*B*)
Cranial (*B*)	−0.070				
	$P = 0.470$				
Cranial (*C*)	**−0.955**	0.033			
	***P*< 0.0001**	$P = 0.732$			
Squamosal (*A*)	**0.780**	−0.084	**−0.763**		
	***P*< 0.0001**	$P = 0.386$	***P*< 0.0001**		
Squamosal (*B*)	−0.097	0.117	0.047	−0.044	.
	$P = 0.317$	$P = 0.227$	$P = 0.625$	$P = 0.648$	
Squamosal (*C*)	**−0.746**	0.080	**0.731**	**−0.935**	−0.058
	***P*< 0.0001**	$P = 0.409$	***P*< 0.0001**	***P*< 0.0001**	$P = 0.547$

Bolded correlations are significant after Bonferroni correction (critical alpha = 0.05/15 = 0.003).

cally different from one another, although *H. erectus* is significantly different from both *H. heidelbergensis* ($P < 0.004$) and *H. sapiens* ($P < 0.001$) (Table 8). *A. afarensis*, *A. africanus*, *P. boisei*, *P. aethiopicus*, and *Homo habilis* were excluded from the one-way ANOVA because these taxa had available sample sizes less than $n = 3$.

Some of the specimens considered as *H. erectus* in this study are attributed elsewhere to *H. ergaster*. As with the craniometric analysis, a two-sample *t*-test was used to determine if there is a significant difference between the means of the African and Asian subsets of the *H. erectus* sample; however, the results of that test indicated that that these groups are not statistically different. This may indicate that these groups do in fact have similar squamosal morphology or may simply be an artifact of the small available sample size, particularly for the African group ($n = 4$). Nevertheless, three of the African specimens (Daka, KNM-ER 3733, and KNM-ER 42700) have the highest and most curved squamosal sutures within the *H. erectus* group, whereas the remaining African specimen (OH 9) has the third least curved squamosal suture.

Correlations between specific polynomial coefficients were tested using a two-tailed Pearson's correlation analysis. Significant correlations (i.e., $P < 0.0001$) were identified between the first (*A*) and third (*C*) coefficients within a given second-order polynomial function, but more importantly, there was a significant correlation between the first and third coefficients of the separate polynomial functions representing cranial and squamosal curvature ($r = 0.780$, $P < 0.0001$) (Table 9). This suggests that these curvatures are highly correlated and that change in one curve will almost certainly produce change in the other.

To clarify the relationship between the squamosal and cranial curvature and the manner in which this relationship varies across taxa, the average of the first polynomial coefficients for squamosal and cranial curvatures were plotted for each taxon. Figure 10 illustrates that the curvature of the squamosal suture increases at a faster rate than cranial curvature. Cranial and squamosal curvatures were either very similar or cranial curvature was greater than squamosal curvature for the great apes, but the degree of squamosal curvature exceeds cranial curvature for all fossil and extant hominin taxa. Within the genus *Homo*, *H. erectus* has the least curved squamosal suture although that taxon is slightly more curved than all *Australopithecus* and *Paranthropus* specimens. Although *H. neanderthalensis* has a higher arched and more curved squamosal suture relative to *H. erectus*, the taxon is noticeably less curved and flatter than *H. heidelbergensis* and *H. sapiens*.

DISCUSSION

The results of the present study suggest that the shape of the temporal squama is variable in both extant and fossil hominids. In the great apes, *Pongo* has a relatively high temporal squama, whereas the squamae of *Pan* and *Gorilla* are flat and unarched. In contrast, the hominin temporal squama is distinct from the great apes, as it is, on average, higher in relation to the roof of the orbit and more curved. Within the fossil sample, there is a general chronological trend toward increasing curvature of the squamosal suture, although there is significant variation in this trend, as evidenced by the decreases in squamosal height and curvature observed in *H. erectus* and *H. neanderthalensis* in relation to their hypothesized ancestors (*H. habilis* and *H. heidelbergensis*, respectively). In *Australopithecus* and *Paranthropus*, the morphology of the temporal squama is highly variable, but all specimens tend to display tall and somewhat arched squamae. In *Homo*, *H. erectus* and Neandertals tend to have the shortest, least arched temporal squamae; however, while the temporal squama morphology of *H. erectus* is relatively variable, specimens attributed to "classic" or Asian *H. erectus* and African *H. erectus* (i.e., *H. ergaster*), cannot be reliably distinguished based on squamosal shape. In addition, Neandertals have the anteroposteriorly narrowest temporal squamae. The temporal squama of *H. heidelbergensis* and *H. sapiens* is the tallest and most curved.

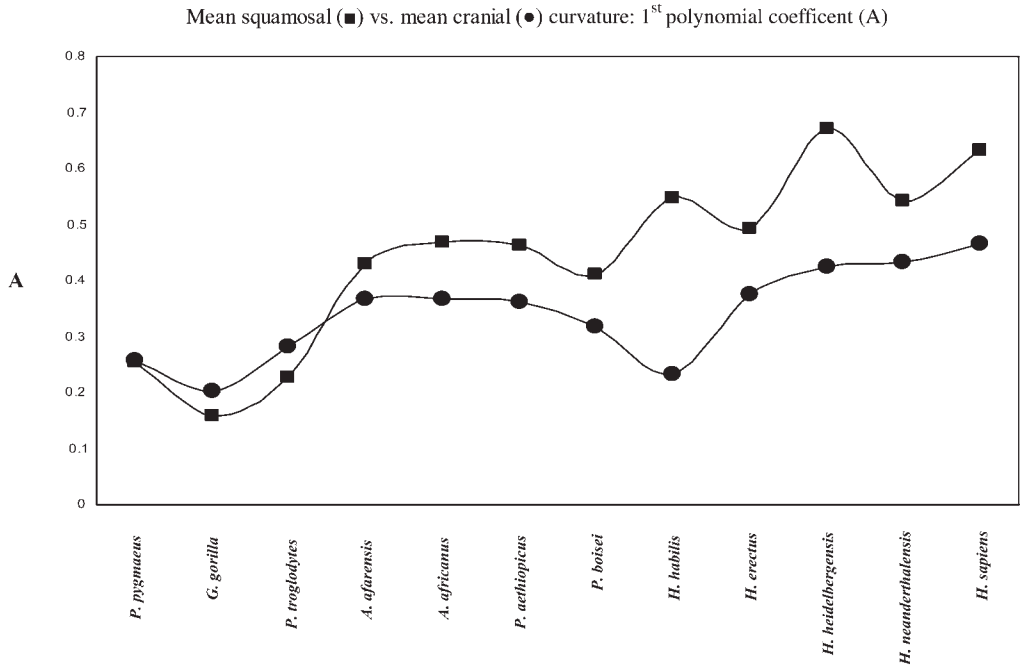

Fig. 10. A plot of mean squamosal and cranial curvature by taxon as represented by the first coefficient (*A*) of the second order polynomial function ($Y = Ax^2 + Bx + C$) defining those curvatures. Note the general increasing trend in squamosal curvature across the samples, and the different relationship between the two curves in the great apes (where the cranial and squamosal curvature values are very similar) as compared to the hominins (where squamosal curvature is greater than cranial curvature in all taxa).

Results of the ANOVAs conducted for the craniometric and HR-PCF analyses suggest that the primary statistical differences in temporal squama morphology are between the apes and the later hominins. In particular, *H. erectus* is statistically significantly different from all of the apes in squama height and curvature. Unfortunately, it is unclear if *H. erectus* is statistically different from the *Australopithecus*, *Paranthropus*, and *H. habilis* samples because of the small number of specimens available from each of these groups.

The correlation analysis examining the variables describing temporal squama and cranial shape further suggests a relationship between overall cranial morphology and the temporal squama. Squama height was found to be significantly positively correlated with overall vault height, and squamosal curvature is significantly correlated with cranial curvature. This suggests that temporal squama form is indeed correlated with cranial vault morphology, although there is a large amount of individual variation within the taxa examined. As a result, variation in temporal squama morphology among taxa seems most likely to be a result of changes in overall cranial morphology, and particularly vault height as it is correlated with increases in cranial capacity.

Character state polarity

Of the great apes, *Pongo* has the tallest and most arched squama, while *Pan* and *Gorilla* have the shortest and least arched squamae, respectively. This difference among the Asian and African great apes is consistent with known differences in facial and cranial architecture (e.g., Shea, 1985, 1986; Lieberman et al., 2000). Most importantly, these differences are not statistically significant, and all the great apes tend to cluster together in the craniometric and curvature analyses, and are therefore distinct from the morphology observed in the hominins. Thus, all of the hominins examined as part of this study display a derived character state in relation to the plesiomorphic condition evident in *Pongo*, *Pan*, and *Gorilla*. In *Australopithecus* and *Paranthropus*, the squama has changed from this plesiomorphic condition such that the squamosal suture is higher on the cranial vault, and its path is more arched. Although no hominin species older than *A. afarensis* were able to be examined as part of this study due to incomplete preservation of the squamosal region, the morphology present in *Australopithecus* and *Paranthropus* may therefore represent a hominin synapomorphy, and minimally was present in the last common ancestor of *Australopithecus* and *Paranthropus*.

Although small sample sizes somewhat prohibit a thorough analysis of the form of the temporal squama in early *Homo*, the data here indicate that the squamosal morphology observed in *H. habilis* is similar to that seen in *Australopithecus* and *Paranthropus*. As a result, the characterization of the long, low, temporal squama of *H. erectus* as a retention of the great ape condition (Andrews, 1984; Martinez and Arsuaga, 1997) is not correct. Although qualitatively similar, the temporal squama morphology observed in *H. erectus* is clearly distinct from the morphology observed in *Pan* and *Gorilla*. Instead, the squama morphology of *H. erectus* appears to be a retention of the hominin plesiomorphic condition, which is a moderately arched, relatively tall temporal squama. The previously described similarity in *H. erectus* and great ape squama morphology is most likely a result of a dramatic increase in cranial length in *H. erectus* without a

corresponding increase in cranial vault height. In comparison, later *Homo* taxa show a trend toward a taller, more curved temporal squama, which is coincident with an increase in cranial height associated with expansion of the parietal bones, and results in the high and arched squamous temporal typical of *H. sapiens*.

Functional implications

As the attachment area for the temporalis muscle, the lateral aspect of the cranial vault, including the temporal squama, is an important component of the masticatory apparatus. However, the functional significance of variation in the shape of the temporal squama is unclear. Rak (1978) and Rak and Kimbel (1991) discussed the significance of the overlap of the temporal bone onto the parietal at the squamosal suture, noting that the overlap at the squamosal suture in *P. boisei* (~25 mm) was considerably larger than in any other species (Rak, 1978). This increased overlap was interpreted as a mechanism to prevent movement of the temporal bones along the squamosal suture. This might occur in the presence of massive anteriorly and laterally placed masticatory muscles, which would tend to slide the temporal bone forward and also lever the temporal squama away from the parietal bone (Rak, 1978). However, little mention was made in regard to the specific shape of the squama, except perhaps in relation to the orientation of the temporalis muscle fibers. Notably, in the analysis here the *Paranthropus* specimens have some of the highest temporal squamae, although they are not the most arched. This result may therefore suggest a relationship between temporal squama shape and overlap that should be explored in more detail, particularly in light of recent research by Byron et al. (2004) suggesting a relationship between masticatory muscle strength and cranial suture complexity.

CONCLUSIONS

Although temporal squama shape is frequently used as a character in analyses of fossil hominins, and a long, low temporal squama is considered diagnostic of *Homo erectus*, the significance of this character in relation to cranial shape has previously been unclear. Furthermore, variation in the shape of the temporal squama in great apes and fossil hominins is little known, and therefore the polarity of this character state has been difficult to define. By quantifying temporal squama shape in a wide cross section of extant and fossil hominids, this study demonstrates that the shape of the temporal squama is highly variable, but that squamosal shape is distinct between extant apes and hominin taxa. These different morphologies are most likely the result of changes in cranial shape related to increased cranial capacity in hominins. This possible relationship suggests that cranial and temporal squama shape may not be independent characters, and their use as such in phylogenetic analyses of fossil hominins (e.g., Martinez and Arsuaga, 1997; Rightmire et al., 2006) should be cautioned. Finally, although the temporal squama of *Homo erectus* is indeed relatively low and unarched, this morphology is distinct from that observed in the great apes, and therefore should not be considered the retention of the great ape condition.

ACKNOWLEDGMENTS

Our thanks to Yohannes Haile-Selassie and Lyman Jellema (Cleveland Museum of Natural History), Dr. Emma Mbua (National Museum of Kenya), and Linda Gordon (Smithsonian National Museum of Natural History) for their assistance and access to extant and fossil collections in their care. This manuscript was improved by comments from Bill Kimbel, Laura Stroik, the editor Christopher Ruff, and three anonymous reviewers.

LITERATURE CITED

Abbate E, Albianelli A, Azzaroli A, Benvenuti M, Tesfamariam B, Bruni P, Cipriani N, Clarke RJ, Ficcarelli G, Macchiarelli R, Napoleone G, Papini M, Rook L, Sagri M, Tecle TM, Torre D, Villa I. 1998. A one-million-year-old *Homocranium* from the Danakil (Afar) depression of Eritrea. Nature 393:458–460.

Andrews P. 1984. An alternative interpretation of the characters used to define *H. erectus*. Cour Forsch-Inst Senckenberg 69:167–175.

Antón SC. 2002. Evolutionary significance of cranial variation in Asian *Homo erectus*. Am J Phys Anthropol 118:301–323.

Antón SC. 2003. Natural History of *Homo erectus*. Yearbk Phys Anthropol 46:126–170.

Asfaw B, Gilbert WH, Beyene Y, Hart WK, Renne PR, WoldeGabriel G, Vrba E, White TD. 2002. Remains of *Homo erectus* from Bouri, Middle Awash, Ethiopia. Nature 416:317–320.

Baba H, Aziz F, Kaifu Y, Suwa G, Kono RT, Jacob T. 2003. *Homo erectus* calvarium from the pleistocene of Java. Science 299:1384–1388.

Brauer G. 1994. How different are Asian and African Homo erectus? Cour Forsch-Inst Senckenberg 171:301–318.

Brauer G, Leakey RE. 1986. The ES-11693 cranium from Eliye Springs, West Turkana, Kenya. J Hum Evol 15:289–312.

Broadfield D, Holloway RL, Mowbray K, Silvers A, Yuan MS, Marquez SC. 2001. Endocast of Sambungmacan 3 (SM 3): a new *Homo erectus* from Indonesia. Anat Rec 262:369–379.

Byron CD, Borke J, Yu J, Pashley D, Wingard CJ, Hamrick M. 2004. Effects of increased muscle mass on mouse sagittal suture morphology and mechanics. Anat Rec 279A:676–684.

Conroy GC, Webber GW, Seidler H, Tobias PV, Kane A, Brunsden B. 1998. Endocranial capacity in an early hominid cranium from Sterkfontein, South Africa. Science 280:1730–1731.

Deane AS, Kremer EP, Begun DR. 2005. A new approach to quantifying anatomical curvatures using High Resolution Polynomial Curve Fitting (HR-PCF). Am J Phys Anthropol 128:630–638.

Delson E, Harvati K, Reddy D, Marcus LF, Mowbray K, Sawyer GJ, Jacob T, Marquez S. 2001. The Sambungmacan 3 *H. erectus Calvaria*: a comparative morphometric and morphological analysis. Anat Rec 262:380–397.

Holloway R. 2000. Brain. In: Delson E, editor. Encyclopedia of human evolution and prehistory. New York: Garland Publishing, p 141–149.

Holloway RL. 1985. The poor brain of *Homo sapiens neanderthalensis*: see what you please. In: Delson E, editor. Ancestors: the hard evidence. New York: Alan R. Liss, p 319–324.

Holloway RL, Shapiro JS. 1992. Relationship of squamosal suture to asterion in pongids (*Pan*): relevance to early hominid brain evolution. Am J Phys Anthropol 89:275–282.

Johanson DC, Edgar B. 1996. From Lucy to language. New York: Simon and Schuster.

Keith A. 1931. New discoveries relating to the antiquity of man. London: W.W. Norton.

Kennedy AR, Sonakia A, Chiment J, Verma KK. 1991. Is the Narmada Hominid an Indian *H. erectus*? Am J Phys Anthropol 86:475–496.

Kimbel WH, Rak Y. 1985. Functional morphology of the asterionic region in extant hominoids and fossil hominids. Am J Phys Anthropol 66:31–54.

Kimbel WH, Rak Y, Johanson DC. 2004. The Skull of *Australopithecus afarensis*. Oxford: Oxford University Press.
Leakey MG, Leakey RE. 1978. Koobi Fora Research Project, Vol. 1: The fossil hominids and an introduction to their context, 1968–1974. Oxford: Clarendon Press.
Lieberman DE, Ross CF, Ravosa MJ. 2000. The primate cranial base: ontogeny, function, and integration. Yearbk Phys Anthropol 43:117–169.
Lockwood CA, Tobias PV. 1999. A large male hominin cranium from Sterkfontein. South Africa, and the status of *Australopithecus africanus*. J Hum Evol 36:637–685.
Macintosh NWG, Larnach SL. 1972. The persistence of *H. erectus* traits in Australian Aboriginal crania. Oceania 7:1–7.
Marquez S, Mowbray K, Sawyer GJ, Jacob T, Silvers A. 2001. New fossil hominid calvaria from Indonesia-Sambungmacan 3. Anat Rec 262:344–368.
Martinez I, Arsuaga JL. 1997. The temporal bones from Sima de los Huesos Middle Pleistocene site (Sierra de Atapuerca. Spain). A phylogenetic approach. J Hum Evol 33: 283–318.
Olivier G, Tisier H. 1975. Determination of cranial capacity in fossil men. Am J Phys Anthropol 43:353–362.
Rak Y. 1978. The functional significance of the squmosal suture in *Australopithecus boisei*. Am J Phys Anthropol 49: 71–78.
Rak Y, Kimbel B. 1991. On the squamosal suture of KNM-WT 17000. Am J Phys Anthropol 85:1–6.
Rightmire GP. 1984. Comparisons of *H. erectus* from Africa and Southeast Asia. Cour Forsch-Inst Senckenberg 69:83–98.
Rightmire GP. 1990. The evolution of *H. erectus*: comparative anatomical studies of an extinct human species. Cambridge: Cambridge University Press.
Rightmire GP, Lordkipanidze D, Vekua A. 2006. Anatomical descriptions, comparative studies and evolutionary significance of the hominin skulls from Dmanisi, Republic of Georgia. J Hum Evol 50:115–141.
Schulter FP. 1976. A comparative study of the temporal bone in three populations of man. Am J Phys Anthropol 44:453–468.
Schultz A. 1915. Form. größe und lage der squama temporalis des menschen. Zeitschrift Morph Anth 19:352–380.
Schwartz JH, Tattersall I. 2003. The human fossil record, Vol. 2: Craniodental morphology of genus *Homo* (Africa and Asia). New York: Wiley-Liss.
Shea BT. 1985. On aspects of skull form in African apes and orangutans, with implications for hominoid evolution. Am J Phys Anthropol 68:329–342.
Shea BT. 1986. On skull form and the supraorbital torus in primates. Curr Anthropol 27:257–260.
Spoor F, Leakey MG, Gathogo PN, Brown FH, Antón SC, McDougall I, Kiarie C, Manthi FK, Leakey LN. 2007. Implications of new early *Homo* fossils from Ileret, east of Lake Turkana, Kenya. Nature 448:688–691.
Stringer CB. 1984. The definition of *Homo erectus* and the existence of the species in Africa and Europe. Cour Forsch-Inst Senckenberg 69:131–143.
Suzuki H, Takai F. 1970. The amud man and his cave site. Tokyo: University of Tokyo Press.
Tobias PV. 1967. Olduvai Gorge: The cranium of Australopithecus (Zinjanthropus) boisei. Cambridge: Cambridge University Press.
Tobias PV. 1985. Single characters and the total morphological pattern redefined: the sorting effected by a selection of morphological features of the early hominids. In: Delson E, editor. Ancestors: the hard evidence. New York: Alan R. Liss, p 94–101.
Vallois H, Billy G. 1965. Nouvelles recherches sur les homes fossils de l'Abri de Cro-Magnon. L'Anthropologie 69:47–74.
Vekua A, Lordkipanidze D, Rightmire Gl-P, Agusti J, Ferring R, Maisuradze G, Mouskhelishvili A, Nioradze M, Ponce de Leon M, Tappen M, Tvalchrelidze M, Zollikofer C. 2002. A new skull of early *homo* from Dmanisi, Georgia. Science 297:85–89.
Walker A. 1994. Early homo from 1.8–1.5 million year deposits at Lake Turkana, Kenya. Cour Forsch-Inst Senckenberg 171:167–173.
Weidenreich F. 1943. The skull of Sinanthropus pekinensis: a comparative odontography of the hominids. Palaeontol Sin D 10:1–484.
White TD, Asfaw B, DeGusta D, Gilbert H, Richards GD, Suwa G, Howell FC. 2006. Pleistocene *Homo sapiens* from Middle Awash, Ethiopia. Nature 423:742–747.
Wood B. 1984. The origins of *H. erectus*. Cour Forsch-Inst Senckenberg 69:99–111.
Wood B. 1991. Koobi Fora Research Project, Vol. 4: Hominid cranial remains. Oxford: Clarendon Press.
Wu X, Poirier F. 1995. Human evolution in China: a metric description of the fossils and a review of the sites. New York: Oxford University Press.